Strong-field theory of four-wave mixing. II. Density-matrix treatment of extra resonances

N. Chencinski, W. M. Schreiber, and A. M. Levine
Department of Applied Sciences, College of Staten Island, C.U.N.Y., Staten Island, New York 10301

Yehiam Prior
Department of Chemical Physics, Weizmann Institute of Science, Rehovot, Israel
(Received 6 February 1990)

A nonperturbative density-matrix formalism is used for the analysis of strong-field four-wave mixing, allowing the treatment of relaxation processes, including lifetime as well as dephasing. The combined role of proper dephasing and level saturation in the generation of extra resonances is studied. It is shown that, whereas in the absence of proper dephasing there is no pressure-induced resonance, there is always a nonzero contribution to the field-induced resonance. For increasing field intensity, a characteristic double saturation is predicted as a function of the field strength. The dependence on the various parameters is investigated, and the conditions under which these effects should be observable are identified.

I. INTRODUCTION

The interaction of strong fields and absorbing molecules manifests itself in many nonlinear optical experiments. Wave mixing is a common example of such interaction, but many others have been investigated since the introduction of strong lasers. The standard theoretical approach to the treatment of problems in nonlinear optics has been the perturbative handling of the strong fields, resulting in a power series expansion of the induced polarization.[1] In this treatment, for a molecular system with a center of inversion (like a free atom or molecule), the loweset-order nonlinear term is of third order. Indeed, the formulation by Bloembergen of nonlinear optics in terms of these susceptibilities has been extremely successful, and most observations may be explained by this "simple" approach.[2] Like any perturbative method, the theory breaks down when the smallness parameter is no longer small, and this occurs when the fields are saturating.

Many situations involving the interaction of strong fields with absorbing molecular level systems have been treated[3–15]. We will not try to provide a full review of the literature, but a partial list of relevant papers was given in our previous paper on the same subject (paper I).[16] The most fundamental problem, a two-level system (TLS) with one strong field, may be handled analytically to all orders in the field, and in essence had been solved by Bloch, who treated material relaxation by including phenomenological rates.[17] When more than two levels are involved, the situation becomes more complicated. A three-level system with two fields may still be treated analytically under certain conditions. However, in practically all treatments of four levels and three input fields, not all fields are allowed to be strong. By far the most common approach is to assume that one of the fields is strong, to solve this problem to all orders, and to treat the other fields as perturbations. Early papers dealing with strong-field interactions were published by Wilcox and Lamb,[8] Bloembergen and Shen,[3] and Freed.[7] More recently Dick and Hochstrasser[9] (DH) published a thorough investigation of strong-field four-wave mixing (FWM). This paper is discussed below. Two very recent papers treating strong-field effects are DeTemple *et al.*[14] who concentrated on resonant frequency tripling, and Oliveira *et al.*[15] who discussed two photon coherences and analyzed destructive interferences between different contributions to the optical polarization.

The observation of the pressure-induced extra resonances[18] (PIER 4) focused attention on the role of relaxation in FWM processes. In these resonances the dephasing process itself, by removing destructive interferences, is responsible for the appearance of additional resonances, and several such resonances had been predicted and observed.[19–21] The perturbation theory description of these resonances is quite adequate for the region where the theory is expected to be valid, namely for weak fields. For stronger fields, as was pointed out by Friedmann and Wilson-Gordon[12] and by Agarwal,[6] the inclusion of orders higher than third will also remove the destructive interference, resulting in an extra resonance. A full review of the dephasing-induced extra resonances has been recently published by Rothberg.[22]

In paper I,[16] we have introduced a strong-field theory of four-wave mixing, based on a wave-function formulation. A transformation to a generalized rotating frame has been used for removal of the fast time dependencies, followed by numerical diagonalization of the time independent Hamiltonian. The paper gives the procedure for identifying the correct Hamiltonian for each of the field permutations, which enabled the study of the particular diagrams giving rise to the PIER 4 extra resonance. In that paper material relaxation processes were not included, the Doppler effect due to molecular velocities was

not included in the calculation, pump depletion was not considered, and each field was assumed to interact with only one pair of levels. Field induced extra resonances were considered in detail, and it was shown that for strong fields, the resonance frequencies are shifted and lines are split.

The paper by Dick and Hochstrasser[9] introduced a density matrix formalism covering both material relaxations and strong fields. DH treated relaxations by including the standard phenomenological rates T_1 and T_2, and in addition, they included incoherent feeding terms as well. In order for the treatment to be self-consistent, they considered a closed system, where the incoherent feeding terms assured that the total population remained constant, and did not decay to zero. The exact solution to the transformed time-independent density-matrix equation was obtained by inverting a 16×16 matrix. To illustrate the formalism, DH considered in detail coherent anti-Stokes and Stokes Raman scattering (CARS and CSRS), but did not include a discussion of the diagrams giving rise to the extra resonances.

In the present paper the formalism developed in DH is used to investigate FWM in general and extra resonances in particular in all regions. The assumptions introduced in paper I are used here as well, with the exception of the inclusion of material relaxation, longitudinal as well as transverse. At low fields, the dominant effect is of the material relaxation, while at high fields it is the fields themselves that give rise to the extra resonances. The intermediate region, where many of the experiments are done, has not been studied previously in any of the above-mentioned papers, and will be treated here.

In addition to FWM, the theory presented here is applicable to any process where several laser beams interact with a few-level system (FLS). Experiments of this kind include multiphoton excitation of atoms and molecules, higher harmonic generation, or the interaction of laser beams with very strong absorbers like semiconductor samples. More generally, the advances in short pulse generation, which have reached pulse lengths of a few femtoseconds, facilitate reasonable experiments with laser intensities hitherto unheard of, and it is expected that perturbation theory approaches will not be valid.

The organization of the paper is as follows. In Sec. II the general formalism is developed, and is applied in Sec. III to a specific group of diagrams of the FWM interaction. In order to avoid confusion due to the level structure of real atoms like Na, we invented a new hypothetical atom, the OLS atom, which has the optimal level structure (OLS) needed to separate the various effects. The OLS atom is defined below, and will be used in this paper. In Secs. IV and V we present results for this atom, and discuss conditions where the effects discussed in this paper may be observed experimentally. The paper concludes with a discussion of the limitations and the direction for further extension of the present theory.

II. GENERAL THEORY

Consider three input laser fields interacting with a four-level system to generate a coherent output field. An energy-level diagram showing a typical interaction is depicted in Fig. 1. Here three input fields of frequencies ω_a, ω_b, and ω_c interact with the four-level molecular system (g,t,k,j) to generate the fourth coherent beam at ω_p $(=\omega_a+\omega_b-\omega_c)$. The standard assumptions of the dipole interaction are made, and the semiclassical treatment is adopted throughout this paper. The system is allowed to undergo material relaxation, which is included in the form of longitudinal and transverse phenomenological rates. The density matrix of the four-level system evolves according to the equation

$$\frac{\partial\rho}{\partial t}=\frac{i}{\hbar}[\rho,H]+(\dot\rho)^R\ . \tag{2.1}$$

The Hamiltonian in Eq. (2.1) is the usual dipole approximation Hamiltonian of interaction of light and matter and the relaxations given by

$$(\dot\rho)^R_{\alpha\alpha}=-\Gamma_\alpha\rho_{\alpha\alpha}+\sum_{\beta=1}^{4}\gamma_{\beta\alpha}\rho_{\beta\beta},\quad \alpha=1,2,3,4 \tag{2.2}$$

$$(\dot\rho)^R_{\alpha\beta}=-\Gamma_{\alpha\beta}\rho_{\alpha\beta},\quad \alpha,\beta=1,2,3,4,\quad \alpha\neq\beta\ . \tag{2.3}$$

In Eqs. (2.2) and (2.3) Γ_α represents longitudinal decay, $\Gamma_{\alpha\beta}$ $(=\Gamma_{\beta\alpha})$ represents transverse decay, and the $\gamma_{\alpha\beta}$ are feeding parameters. Since the present theory deals with strong fields, one may not make the assumption that the population in the ground state remains constant, as is usually done in the conventional perturbation theory of the third-order susceptibility $\chi^{(3)}$. Instead, the assumption is made that the system is closed, with feeding terms chosen accordingly. The requirement that the system be closed means that $\mathrm{Tr}(\rho)=1$, or $\mathrm{Tr}(\dot\rho)^R=0$. The condition on the connection between the relaxation rates and the feeding terms is

$$\Gamma_\alpha=\sum_{\beta=1}^{4}\gamma_{\alpha\beta},\quad \alpha=1,2,3,4\ . \tag{2.4}$$

For an actual atomic (molecular) system Eq. (2.4) means that there is neither relaxation away from the four-level system nor feeding from the outside world. In a more general treatment this strong condition could be relaxed somewhat, but the condition of $\mathrm{Tr}(\rho)=1$ should be maintained.

In order to remove the fast time dependence of the in-

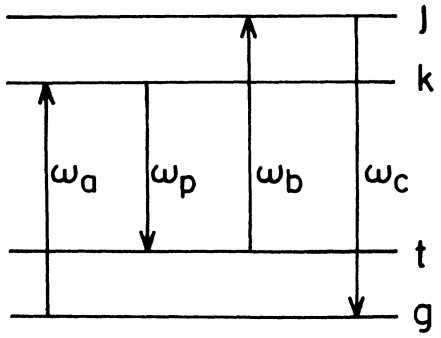

FIG. 1. An energy level diagram describing the interaction of three strong fields with a four-level system.

put fields, and in a way completely analogous to the transformation to a rotating frame of the two-level system, one may use the same unitary diagonal transformation matrix $T(t)$ which was defined in paper I, and apply it to the Liouville equation (2.1). For illustrative purposes the two-level problem is treated in Appendix A, where the connection between the density-matrix and the wave-function approaches is made.

Thus, from the transformation

$$\rho' = T\rho T^{\dagger} \tag{2.5}$$

the resulting equation is

$$\frac{\partial \rho'}{\partial t} = \frac{i}{\hbar}[\rho', H'] + T(\dot{\rho})^R T^{\dagger} , \tag{2.6}$$

where in Eq. (2.6) the transformed Hamiltonian is given by

$$H' = THT^{\dagger} + i\hbar \dot{T} T^{\dagger} \tag{2.7}$$

The transformed time-independent Hamiltonian H' is the same as that of our wave-function treatment in paper I. In component form, Eq. (2.6) will look like

$$\frac{\partial \rho'_{ii}}{\partial t} = -\frac{i}{\hbar}\sum_{r=1}^{4} H'_{ir}\rho'_{ri} + \frac{i}{\hbar}\sum_{r=1}^{4} H'_{ri}\rho'_{ir} - \Gamma_i \rho'_{ii} + \sum_{q=1}^{4} \gamma_{qi}\rho'_{qq} \quad \text{for } i = 1,2,3,4 \tag{2.8}$$

$$\frac{\partial \rho'_{im}}{\partial t} = -\frac{i}{\hbar}\sum_{r=1}^{4} H'_{ir}\rho'_{rm} + \frac{i}{\hbar}\sum_{r=1}^{4} H'_{rm}\rho'_{ir} - \Gamma_{im}\rho'_{im} \quad \text{for } i,m = 1,2,3,4, \quad i \neq m . \tag{2.9}$$

The elements of the transformation matrix $T(t)$ are of the form

$$T_{ij}(t) = e^{i\phi_i t}\delta_{ij}, \quad i,j = 1,2,3,4 \tag{2.10}$$

where ϕ_i is a linear combination of the three incident frequencies. Thus $\rho_{ii} = \rho'_{ii}$, and $\rho_{im} = \rho'_{im}\bar{T}_{ii}T_{mm}$ for $(i,m = 1,2,3,4)$. Equations (2.8) and (2.9) can be expressed in a matrix form

$$\frac{\partial \rho'}{\partial t} = -iX\rho' , \tag{2.11}$$

where the matrix X is a time-independent supermatrix which has the dimensionality 16×16. The matrix ρ' is a column vector of dimension 16 whose elements are 16 ρ'_{ij}. The choice of the order of the elements is somewhat arbitrary within each calculation, and here we choose the following convention:

$$\rho'_{11}, \rho'_{22}, \rho'_{33}, \rho'_{44} \quad \text{for rows } 1-4 , \tag{2.12}$$

$$\rho'_{12}, \rho'_{13}, \rho'_{14}, \rho'_{23}, \rho'_{24}, \rho'_{34} \quad \text{for rows } 5-10 , \tag{2.13}$$

$$\rho'_{21}, \rho'_{31}, \rho'_{41}, \rho'_{32}, \rho'_{42}, \rho'_{43} \quad \text{for rows } 11-16 . \tag{2.14}$$

Note that since $\rho'_{ij} = \bar{\rho}'_{ji}$, rows 11–16 are the complex conjugate of rows 5–10, respectively. Equation (2.11) can be solved by the Laplace transform method subject to the initial values $\rho'(0)$, yielding the steady-state solution ρ'^{s} upon letting $t \to \infty$.

From Eq. (2.11), the steady-state solution ρ'^{s} satisfies the condition

$$X\rho'^{s} = 0 . \tag{2.15}$$

By construction, since the first four equations in Eq. (2.15) are linearly dependent, the matrix X is singular. In order to remove this singularity, replace the first of these equations by requiring

$$\mathrm{Tr}\rho'^{s} = 1 . \tag{2.16}$$

The result of using this constraint is a set of 16 equations which may be written in matrix form, in the same way as in paper I:

$$Z\rho'^{s} = R , \tag{2.17}$$

where the matrix Z (given in Appendix B) is obtained from the matrix X by replacement of the first row with 1's at the first four positions and zeros at the other positions. The matrix R is a column vector of 16 rows whose only nonzero element is a 1 in the first row, $R_i = \delta_{i1}$ for $i = 1, \ldots, 16$. For the selection rules implied by Fig. 1 the structure of the transformed Hamiltonian H' is

$$H' = \hbar \begin{pmatrix} h_{11} & 0 & h_{13} & h_{14} \\ 0 & h_{22} & h_{23} & h_{24} \\ \bar{h}_{13} & \bar{h}_{23} & h_{33} & 0 \\ \bar{h}_{14} & \bar{h}_{24} & 0 & h_{44} \end{pmatrix} . \tag{2.18}$$

The expectation value of any operator O is given by

$$\langle O \rangle = \mathrm{Tr}[O\rho(t)] = \sum_{i=1}^{4}\sum_{k=1}^{4} O_{ik}\rho'_{ki}(t)T_{ii}(t)\bar{T}_{kk}(t) . \tag{2.19}$$

Commensurate with the selection rules implied by Fig. 1, one may represent the polarization operator:

$$P = \begin{pmatrix} 0 & 0 & p_{13} & p_{14} \\ 0 & 0 & p_{23} & p_{24} \\ \bar{p}_{13} & \bar{p}_{23} & 0 & 0 \\ \bar{p}_{14} & \bar{p}_{24} & 0 & 0 \end{pmatrix} . \tag{2.20}$$

From Eq. (2.19), the steady-state expectation value of the polarization is

$$\langle P_s \rangle = \sum_{i=1}^{4}\sum_{k=1}^{4} P_{ik}\rho'^{s}_{ki}T_{ii}(t)T_{kk}(t) . \tag{2.21}$$

It is important to remember that the interaction of four fields with a four-level system involves many permutations of the order of the interacting fields, as represented by the 48 terms in the full expression for the third-order susceptibility $\chi^{(3)}$, or as may be seen from a diagrammatic description of the interaction. These terms separate into 12 parametric diagrams, and 12 sets of three nonparametric diagrams. Each parametric diagram, and each set of three nonparametric diagrams correspond to a

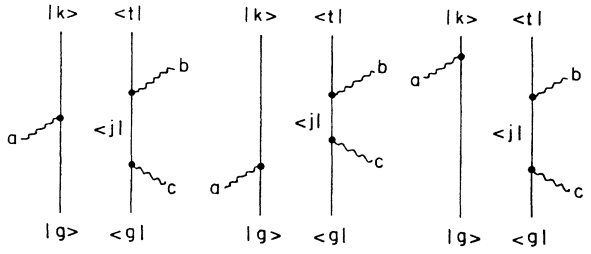

FIG. 2. A set of three nonparametric diagrams describing (to lowest order) the interaction calculated in this paper. These diagrams are known to give rise to PIER 4.

separate Hamiltonian, as detailed in paper I. The use of these diagrams does not imply a perturbation calculation, as they are used only for bookkeeping purposes. In the present paper one such triplet is treated in detail, and the extension to all others is straightforward. Figure 2 gives the diagrams treated in this paper, which correspond to diagrams 31, 32, and 33 in the notation of Prior.[23]

From Eq. (2.21), one may extract the Fourier component of the polarization at the frequency ω_p $(=\omega_a+\omega_b-\omega_c)$ where $\omega_a,\omega_b,\omega_c$ are the frequencies of the three incident fields, respectively. This can be done by choosing i and k such that

$$T_{il}(t)\bar{T}_{kk}(t)=e^{-i\omega_p t}, \tag{2.22}$$

which implies the following choice for the various diagrams (as designated in paper I): $i=1$, $k=4$ for the first set of parametric diagrams (1–6); $i=3$, $k=1$ for the second set of parametric diagrams (7–12); $i=4$, $k=2$ for the first set of nonparametric diagrams (13–30); $i=2$, $k=3$ for the second set of nonparameteric diagrams (31–48). From Eq. (2.21) the respective polarization components at ω_p are

$$P_{\omega_p}=\begin{cases} p_{14}\rho'^{s}_{41} & \text{for diagrams 1–6}, \\ \bar{p}_{13}\rho'^{s}_{13} & \text{for diagrams 7–12}, \\ \bar{p}_{24}\rho'^{s}_{42} & \text{for diagrams 13–30}, \\ p_{23}\rho'^{s}_{32} & \text{for diagrams 31–48}. \end{cases} \tag{2.23}$$

III. APPLICATION OF THE THEORY

The formulation of the problem in Sec. II was in general terms, and is applicable to any interaction. In order to illustrate the results obtained from the theory, we apply it to the nonparametric diagrams 31–33, see Fig. 2. These diagrams had been treated in the past, and are known to give rise to PIER 4. In the general formalism, all four fields may be strong. In most experimental situations, however, the generated field may be assumed to be weak, and therefore we make this assumption at this point. As a result, there are only three nonzero fields included in the Hamiltonian:

$$H=\hbar\begin{bmatrix} 0 & 0 & \bar{V}_b e^{i\omega_b t} & \bar{V}_c e^{i\omega_c t} \\ 0 & \omega_{tg} & 0 & \bar{V}_a e^{i\omega_a t} \\ V_b e^{-i\omega_b t} & 0 & \omega_{kg} & 0 \\ V_c e^{-i\omega_c t} & V_a e^{-i\omega_a t} & 0 & \omega_{jg} \end{bmatrix}, \tag{3.1}$$

where $\omega_{lm}=(E_l-E_m)/\hbar$ for $l,m=g,t,k,j$, and V_s $(s=a,b,c)$ is the strength of the atom-field interaction, which includes the field strength and the dipole moment of the appropriate transition.

Referring to Eq. (2.7), the transformation matrix

$$T=\begin{bmatrix} e^{ia_1 t} & 0 & 0 & 0 \\ 0 & e^{ia_2 t} & 0 & 0 \\ 0 & 0 & e^{ia_3 t} & 0 \\ 0 & 0 & 0 & e^{ia_4 t} \end{bmatrix} \tag{3.2}$$

when applied to the Hamiltonian in Eq. (3.1) yields

$$H'=\hbar\begin{bmatrix} D_1 & 0 & \bar{V}_b & \bar{V}_c \\ 0 & D_2 & 0 & \bar{V}_a \\ V_b & 0 & D_3 & 0 \\ V_c & V_a & 0 & D_4 \end{bmatrix}, \tag{3.3}$$

where the linear combinations of frequencies for the transformation are

$$\begin{aligned} a_1&=\tfrac{1}{2}(\omega_a-\omega_b-\omega_c), \\ a_2&=-\tfrac{1}{2}(\omega_a+\omega_b-\omega_c), \\ a_3&=\tfrac{1}{2}(\omega_a+\omega_b-\omega_c), \\ a_4&=\tfrac{1}{2}(\omega_a-\omega_b+\omega_c), \end{aligned} \tag{3.4}$$

and in Eq. (3.3) the following quantities are defined:

$$\begin{aligned} D_1&=-a_1, \\ D_2&=\omega_{tg}-a_2, \\ D_3&=\omega_{kg}-a_3, \\ D_4&=\omega_{jg}-a_4. \end{aligned} \tag{3.5}$$

The solution for ρ'^{s} is found from Eq. (2.17). From Eq. (2.23) the component of the polarization at ω_p is

$$P_{\omega p}=p_{tk}\rho'^{s}_{kt} \tag{3.6}$$

Explicit results for the OLS atom are presented in Sec. IV.

IV. NUMERICAL RESULTS

The formulation described in Sec. III allows for a wide range of parameters, including three arbitrary field strengths, three arbitrary detuning, and arbitrary pressure-induced dephasing. This wealth of generality is also a curse; it makes it very difficult to anticipate all of the physically interesting regimes that one may wish to study. To unravel this detail, and separate the various

effects, the OLS atom is used. Thus, in all of the numerical work presented $\omega_{tg}=500\ \text{cm}^{-1}$, $\omega_{kg}=10\,000\ \text{cm}^{-1}$, and $\omega_{jg}=11\,000\ \text{cm}^{-1}$.

In paper I, both the OLS atom and sodium were studied, with no fundamental difference observed in the physical explanations. In the figures that follow the polarization is plotted in units of the dipole moment of the transition coupled to the generated wave ω_P.

In the current paper both spontaneous decay (T_1) and (pressure-induced) proper dephasing (T_2) are included. The spontaneous decay is described by a phenomenological rate Γ_{SE} to represent the spontaneous emission decay from the upper atomic levels (k and j) to the ground state g. The off-diagonal dephasing has been taken to be

$$\Gamma_{lm}=\tfrac{1}{2}(\Gamma_l+\Gamma_m)+\alpha P\ ,$$

where α is a constant of proportionality and P is the pressure.

The logical first case to examine is an ordinary resonance. For the diagrams given in Fig. 2, the two ordinary resonances occur at $\omega_c=\omega_{tg}+\omega_b$ and at $\omega_c=\omega_{jg}$. In Fig. 3, the real and imaginary parts of the ω_p component of the induced polarization are shown as a function of ω_c as it sweeps through the ordinary resonance near ω_{jg}, for a fixed detuning of the V_a field ($\Delta\omega_a=\omega_a-\omega_{kg}$). The pressure used in calculating these expressions was chosen such that $\Gamma_{jg}=\Gamma_{SE}$ (namely, $\alpha P=\Gamma_{SE}/2$), but varying the pressure produced similar results.

The "weak" V_c field case ($V_c/\Gamma_{SE}=0.1$), shown in Fig. 3(a), has a resonance shape similar to traditional perturbation theory. The peak-to-peak variation of the real part is equal to the peak of the imaginary part, and the half-width of the resonance is Γ_{jg}. Raising the pressure to increase the proper dephasing increased the width of the resonance in this "weak-field" case, as predicted by perturbation theory. The shift observed in the resonance frequency is due to the strong V_a field. This Stark shift is given[24] in the limit of $\Gamma_{SE}\ll V_a\ll|\Delta\omega_a|$ by $V_a^2/\Delta\omega_a$. It may be described in the "dressed-atom" picture, as the shift of the dressed levels away from the "bare-atom" energy levels.

Increasing the strength of the field V_c, whose frequency is swept through the resonance, suppresses the relative magnitude of the imaginary part, as shown in Fig. 3(b). The strong-field case ($V_c/\Gamma_{SE}=10$) is shown in Fig. 3(c), where the resonance has only a small imaginary part and the width is determined only by the power broadening. In a manner analogous to the two-level system, a saturating field will equalize the populations, will reduce the on-resonance imaginary part of the induced polarization to zero, and will cause the peak-to-peak amplitude of the real part to be field independent. In what follows, a resonance line where the real and imaginary parts are of equal amplitudes will be referred to as having a "perturbativelike" line shape, while the case of a suppressed imaginary part will be described as having a "strong-field" line shape. For the rest of the paper, the real amplitude is defined as the peak-to-peak variation of the real part of the polarization and the imaginary amplitude is defined as the peak to background variation of the imaginary part of the polarization. It is understood that if the resonance occurs at a shifted position, the amplitudes are found at the new position of the resonance.

The variation of the real and imaginary amplitudes of

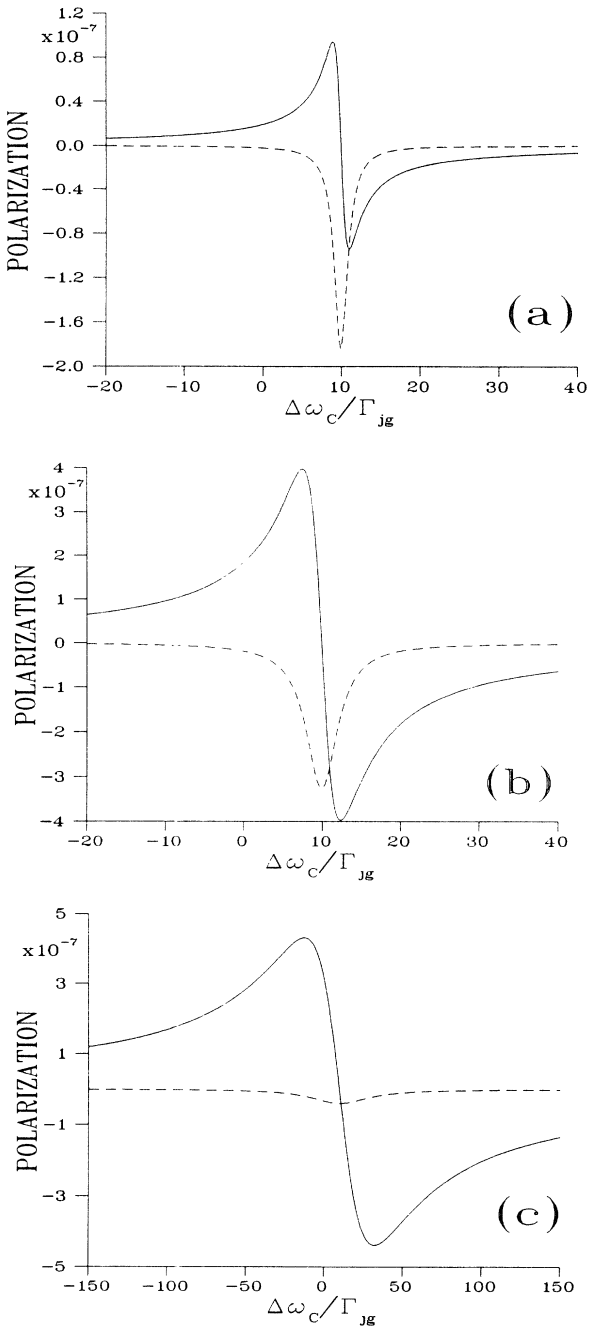

FIG. 3. The real (solid line) and imaginary (dashed line) parts of the Fourier component of the induced polarization at ω_P as a function of $\Delta\omega_c$ ($=\omega_c-\omega_{jg}$). In this and all subsequent figures $\Gamma_{SE}=0.0001\ \text{cm}^{-1}$. Here $\Delta\omega_a=-0.1\ \text{cm}^{-1}$, $V_a=0.01\ \text{cm}^{-1}$. The frequency axis is normalized to the linewidth Γ_{jg} ($=\Gamma_{SE}$ for this pressure). (a) A weak V_c field ($V_c/\Gamma_{SE}=0.1$). The resonance is Stark shifted by the strong V_a field ($V_a/\Gamma_{SE}=100$); (b) An intermediate V_c field ($V_c/\Gamma_{SE}=1.0$); (c) A strong V_c field ($V_c/\Gamma_{SE}=10.0$).

the resonance as a function of the logarithm of V_c (for a given fixed V_a) is depicted in Fig. 4(a). For $V_c \ll \Gamma_{SE}$, perturbation theory holds and the amplitudes are equal and proportional to V_c. The usual saturation sets in at $V_c \simeq \Gamma_{SE}$ leaving a real part whose peak amplitude is constant with increasing V_c, and causing the imaginary part to fall off as $1/V_c$ consistent with the analysis of the two-level system.

The dependence of the four-wave mixing signal on V_a for strong and weak V_c is shown in Figs. 4(b) and 4(c). In the case of a weak V_c field [Fig. 4(b)] perturbation theory holds as long as $V_a < \Delta\omega_a$ where the FWM signal becomes V_a independent. The line shapes remain perturbativelike in the entire range of V_a (i.e., the imaginary and real amplitudes are equal). For V_c strong enough to saturate the *jg* transition, the V_a dependence is shown in Fig. 4(c). Both the real and imaginary amplitudes become V_a independent when $V_a > \Delta\omega_a$, but the imaginary part is smaller than the real part, exhibiting "strong-field-like" line shapes. Since the V_c field is interacting only with the *jg* transition it is not surprising that this interaction is described by the two-level theory. The line shape is determined only by V_c, regardless of the size of V_a.

Extra resonances had been discussed previously in the context of perturbation theory,[18,22] and their behavior may be described in those terms. The predicted feature of these resonances is a linear dependence of the resonance amplitude on the pressure, and an inverse quadratic dependence on the detuning $\Delta\omega_a$. As is inherent in perturbation theory, there is a linear dependence on each of the fields V_a, V_b, and V_c.

In paper I, the ordinary resonance at $\omega_c = \omega_{jg}$ was shown to be part of a Rabi pair with the "extra resonance" at $\omega_c = \omega_a + \omega_{jk}$. For low fields, the amplitude of the extra resonance is much smaller than that of the ordinary resonance, so only the latter is observed. As V_a is increased (for a fixed nonzero $\Delta\omega_a$) the "extra" field-induced resonance (FIRE) may be observed. At very high fields ($V_a \gg \Delta\omega_a$) the two peaks are of equal amplitude, are separated by twice the Rabi frequency, and there is no distinction between them. Note that in the absence of proper dephasing, there is no pressure-induced extra resonance, whereas there is always a field-induced resonance. In what follows, the combined effect of the field (FIRE) and pressure induced (PIER) extra resonances is studied.

The transition between PIER and FIRE is established in Fig. 5. The dependence of the real amplitude on the pressure is displayed on a log-log plot for small V_a at different values of V_c. For small V_c ($V_c \ll \Gamma_{SE}$) the linear dependence on pressure is clearly seen. The actual curve including the saturation at high pressure is identical to the standard perturbation theory description of PIER 4. As V_c is increased one observes regions where the amplitude is pressure independent. Changing V_c from $10\Gamma_{SE}$ to $100\Gamma_{SE}$ increases the amplitude by three orders of magnitude, showing a marked nonlinear dependence on V_c. In this region, the resonance can be identified as the field-induced resonance which had been discussed in paper I. For any given input field intensity,

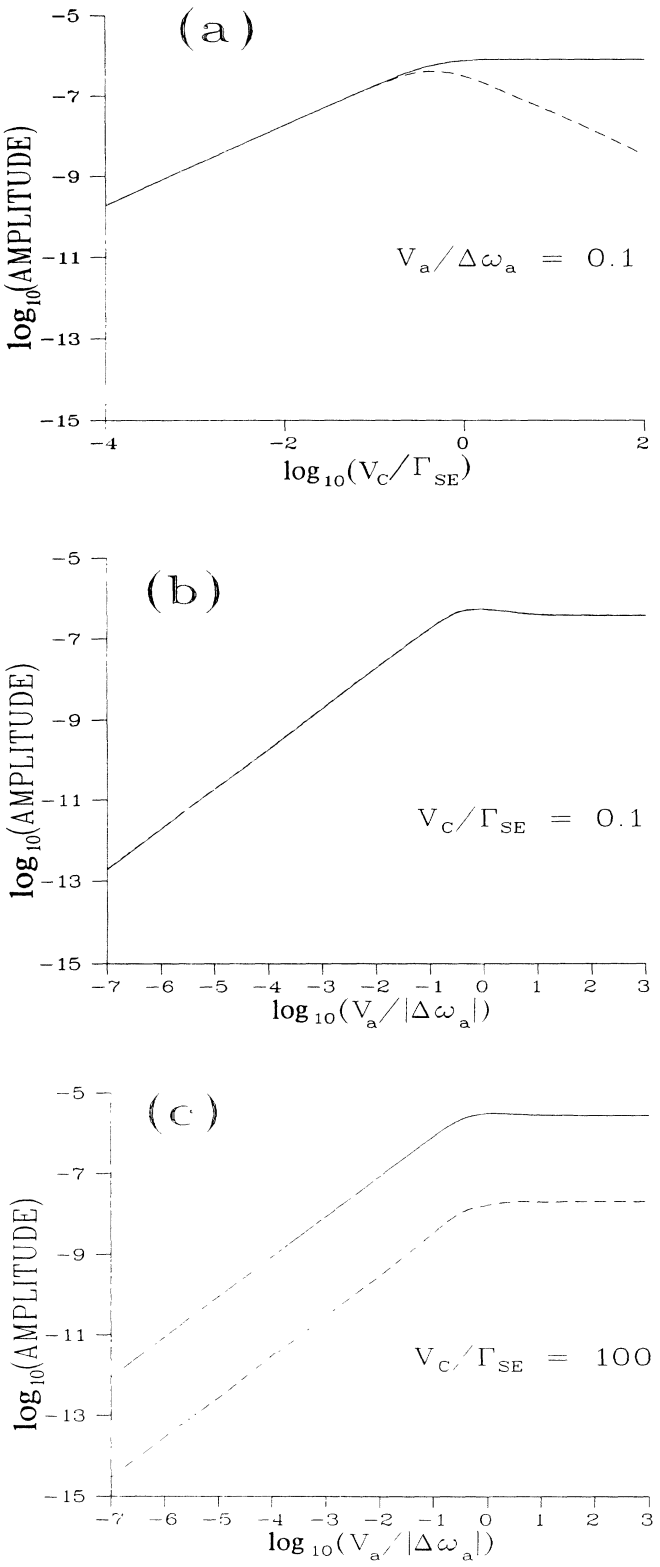

FIG. 4. The real (solid line) and imaginary (dashed line) parts of the amplitude as a function of field strength for an ordinary resonance. The conditions are $\Delta\omega_a/\Gamma_{SE} = -1000$ and $\Gamma_{jg} = \Gamma_{SE}$. In this, and in all subsequent figures, a log-log plot is used. (a) Amplitude vs V_c/Γ_{SE}, with $V_a/|\Delta\omega_a| = 0.1$; (b) Amplitude vs $V_a/|\Delta\omega_a|$, with $V_c/\Gamma_{SE} = 0.1$; (c) Amplitude vs $V_a/|\Delta\omega_a|$, with $V_c/\Gamma_{SE} = 100$.

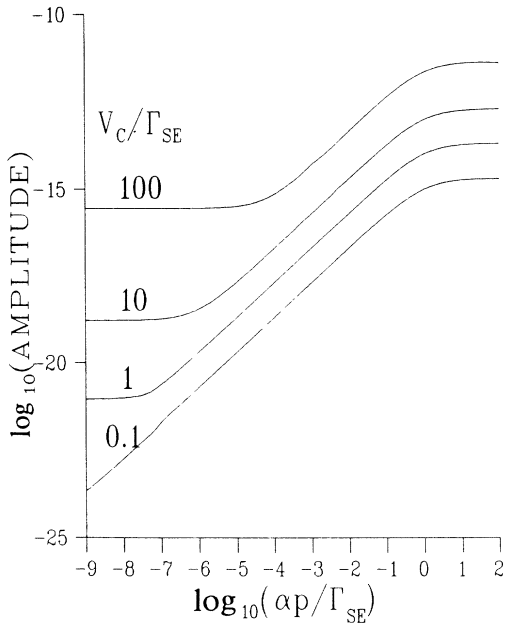

FIG. 5. The pressure dependence of the real amplitude of the extra resonance. The conditions are $V_a/\Gamma_{SE}=0.01$ and $\Delta\omega_a/\Gamma_{SE}=-1000$. The four curves shown are for different values of V_c/Γ_{SE}, as indicated.

there exists a pressure low enough so that the region of FIRE may be reached.

Choosing a value of V_c where the transition between PIER and FIRE is readily apparent ($V_c=10\Gamma_{SE}$), the dependence of amplitude on V_a and its detuning $\Delta\omega_a$ can be studied. Figure 6(a), computed for a pressure where the proper dephasing is equal to $\Gamma_{SE}/2$, shows a linear dependence of the real amplitude on V_a for low values of V_a. Varying the detuning $\Delta\omega_a$ reveals an inverse quadratic dependence on $\Delta\omega_a$ in agreement with traditional perturbation theory. At higher values of V_a, a transition to a region where the amplitude increases faster than linearly is clearly observed. Further increases in V_a produce saturation for values of $V_a>\Delta\omega_a$. The regions linear in V_a exhibit perturbative line shapes (the equal imaginary amplitude is not shown), whereas the saturating region exhibits "strong-field-like" line shapes. Figure 6(b), computed under the same conditions as Fig. 6(a) except that the proper dephasing has been reduced by five orders of magnitude, shows the FIRE behavior. At low V_a, a linear dependence on V_a is indeed observed, but decreasing $\Delta\omega_a$ by one order of magnitude increases the amplitude by four orders of magnitude, a behavior not predicted by traditional perturbation theory. As in Fig. 6(a), higher values of V_a lead to a region where the amplitude is nonlinear in V_a, up to saturation for $V_a>\Delta\omega_a$. As long as V_a is small compared to $\Delta\omega_a$ "perturbativelike" line shapes are observed.

Figures 6(a) and 6(b) were computed at moderate V_c ($V_c=10\Gamma_{SE}$). Under these conditions the strong field is V_a, and the V_c field can be thought of as a perturbation around it. The situation becomes more complicated for strong V_c ($V_c=10^3\Gamma_{SE}$) as shown in Figs. 6(c) and 6(d). The linear dependence on V_a reaches a plateau before the nonlinear V_a region is reached, producing a curve with two "saturation" regions. The first plateau starts at a field intensity that is pressure independent but depends on the $\Delta\omega_a$ detuning. For $\Delta\omega_a<V_c$, a single plateau is observed, displaying a "universal" saturation that does not depend on any of the parameters (except for V_b and its detuning)

Next we consider the dependence of the real amplitude on V_a and V_c in the various FIRE regions. Figure 7(a) depicts the situation for a very small proper dephasing rate $\alpha P=10^{-5}\Gamma_{SE}$. (This rate is artificially small, and was chosen to illustrate the dependence.) In this figure the logarithm of the amplitude is shown as a function of the logarithm of V_a for different values of V_c. For $V_a<\Gamma_{SE}$ and $V_c<\Gamma_{SE}$, the amplitude is linear in V_a and V_c [also linear in pressure and quadratic in $(\Delta\omega_a)^{-1}$, not shown in the figure] which is the traditional PIER 4 behavior. In the intermediate region ($\Delta\omega_a\gg V_a\gg\Gamma_{SE}$) the amplitude is a nonlinear function of V_a exhibiting a fifth-power dependence on V_a. For strong V_a ($V_a>\Delta\omega_a$) the curves saturate in the same fashion as discussed in Fig. 6, displaying the "universal" saturation.

Figure 7(b) is analogous to Fig. 7(a), for the V_c field. The same arguments apply, but in addition the asymmetry between the two is seen by the decline of the FWM amplitude at large V_c levels. As discussed below, the strength of the V_c field determines the ground-state level shift, determining the intensity required to saturate the *jg* transition. When V_a is increased further such that it is greater than V_c, the roles are reversed, and the level shift is determined by V_a. The amplitude exhibits a nonlinear region, finally saturating [as in Fig. 6(a)] when $V_a>\Delta\omega_a$. If $V_c>\Delta\omega_a$ the amplitude has only a single saturation as shown by the top curves. In both figures, the dependence on the weaker field may be seen by looking at the parameter describing each curve. Thus, in Fig. 7(a), as V_c changes from 10^{-7} to 1, the incremental increase in the signal changes from linear at low values ($V_c<\Gamma_{SE}$) to higher than linear at moderate values, and eventually it decreases (not shown) for very high values ($V_c>\Delta\omega_a$). This last behavior pattern is shown explicitly in Fig. 7(b), and is discussed below. Figures 7(c) and 7(d) repeat the condition of Figs. 7(a) and 7(b) for a higher proper dephasing rate ($\alpha P=\Gamma_{SE}/2$). The qualitative behavior is the same except that the PIER 4 region moves up by the appropriate factor, without significantly affecting the FIRE region.

V. DISCUSSION

The analysis of saturation in a two-level system is relatively straightforward. The criterion for saturation is whether the field strength is larger or smaller than a properly defined saturation parameter which depends on the dephasing rate and the detuning. Close to resonance, the dominant contribution to the saturation parameter is the dephasing rate (T_2 in the two-level notation), but at larger detunings the dominant contribution is from the

detuning. More specifically the dependence is on $(\Delta\omega_a^2+\Gamma^2)^{1/2}$, so the well-known result is that it is more difficult to saturate a transition if the saturating field is tuned off resonance.[17] In a four-wave mixing interaction involving strong fields, the situation is more complicated. A strong field, in addition to saturating its own transition, causes level shifts increasing or decreasing the apparent detunings of other fields, and thus affecting their saturation levels. In the cases illustrated in Figs. 5–7 V_b is detuned away from resonance, is nonsaturating, and therefore the situation may be analyzed in terms of a three-level system with two strong fields.

The three levels involved are the g, j, and k levels in Fig. 1, and the two fields are the V_a and V_c fields. These two fields are not equivalent, as the ω_c is swept through resonance while ω_a is fixed for a given experiment. The two fields interact with the ground state g, and therefore if either one is strong, it will effect the other one through the level shift of the ground state. In what follows the different cases where one or both fields are strong are discussed.

The standard dressed atom picture treats the case of one strong field. Since here more than one field is present, the order of dressing the levels is not *a priori* clear, and should be defined for each case, depending on the strength of the fields involved. If one of the fields (V_a or V_c) is much stronger than the other, the situation is obvious, the strong field dresses the levels while the weaker one induces transitions between the dressed levels. If both fields are strong, the dressing is less trivial. For each field three regions may be defined: weak ($V \ll \Gamma$), moderate (detuning $\gg V \gg \Gamma$), and strong ($V \gg$ detuning, $V \gg \Gamma$). The unique situation in the FWM experiment is that the c field is scanned through resonance, and therefore its relevant detuning always vanishes, and the extra resonance transition is always saturated by the V_c field as long as $V_c > \Gamma_{SE}$.

When level shifts are considered, however, another consideration enters. The frequency of the V_a field is fixed, and therefore this field should be considered with its inherent detuning $\Delta\omega_a$. If the c field is strong, it causes the ground level to shift, reducing the detuning of the a field. Thus, the relevant criterion is whether the c field is capable of shifting the ground state into resonance with the a field. At a certain V_c strength, the c field shifts the ground state to a complete resonance with the a field, and under these conditions the saturation of the jg transition is the easiest, requiring the lowest V_a. If V_c is increased further ($V_c > \Delta\omega_a$), the level is shifted through and away from resonance, making it more difficult to saturate. This accounts for the behavior observed in Figs. 7(b) and 7(d) where increasing V_c decreases the ampli-

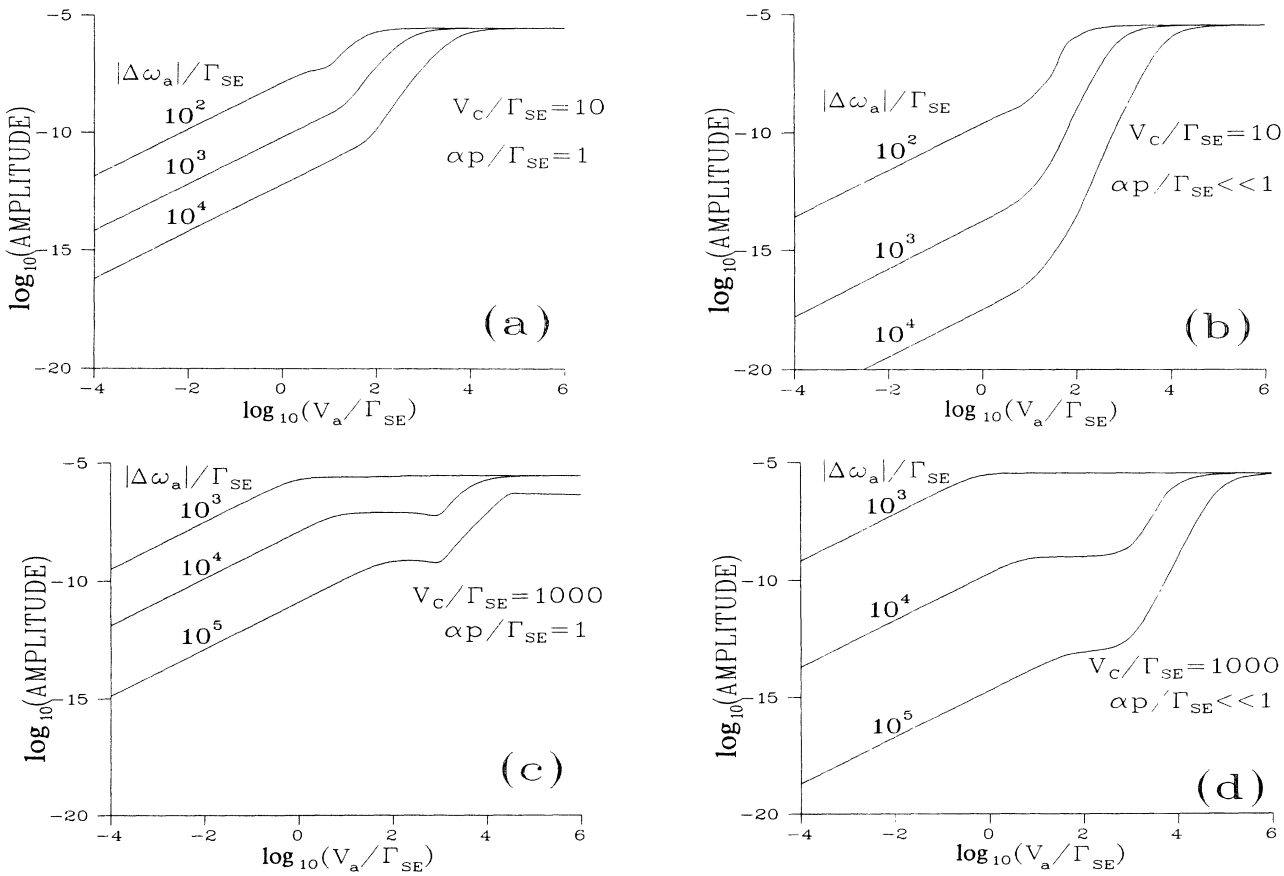

FIG. 6. The dependence of the real amplitude on field strength V_a for different values of the detuning $\Delta\omega_a$. (a) Moderate proper dephasing, moderate V_c; (b) Very low proper dephasing, moderate V_c; (c) Moderate proper dephasing, strong V_c; (d) Very low proper dephasing, strong V_c.

tude. With increasing V_c, the strength of V_a needed to achieve the universal saturation is lower, until at $V_c > \Delta\omega_a$ the FWM signal drops indicating level shifts that are too large for V_a to compensate. Thus, under these circumstances, the relevant detuning for the definition of a strong V_c field is $\Delta\omega_a$. In all other cases, detuning stands for the properly defined frequency difference between the laser frequency and the shifted level frequency.

The dressing of a state by strong fields is a convenient way to discuss the case of one strong and one weak field. Consider first the situation of a strong V_a and a weak V_c. Here one may analyze the situation by dressing the levels by the a field, and continuing the discussion from the split g and k levels after the proper superposition was imposed on them by the dressing process. Thus, the effect of the a field is to shift the levels, and to determine the population of the two split ground states. In accordance with the standard dressed state theory,[25] the population of the two levels is determined by the strength of the field

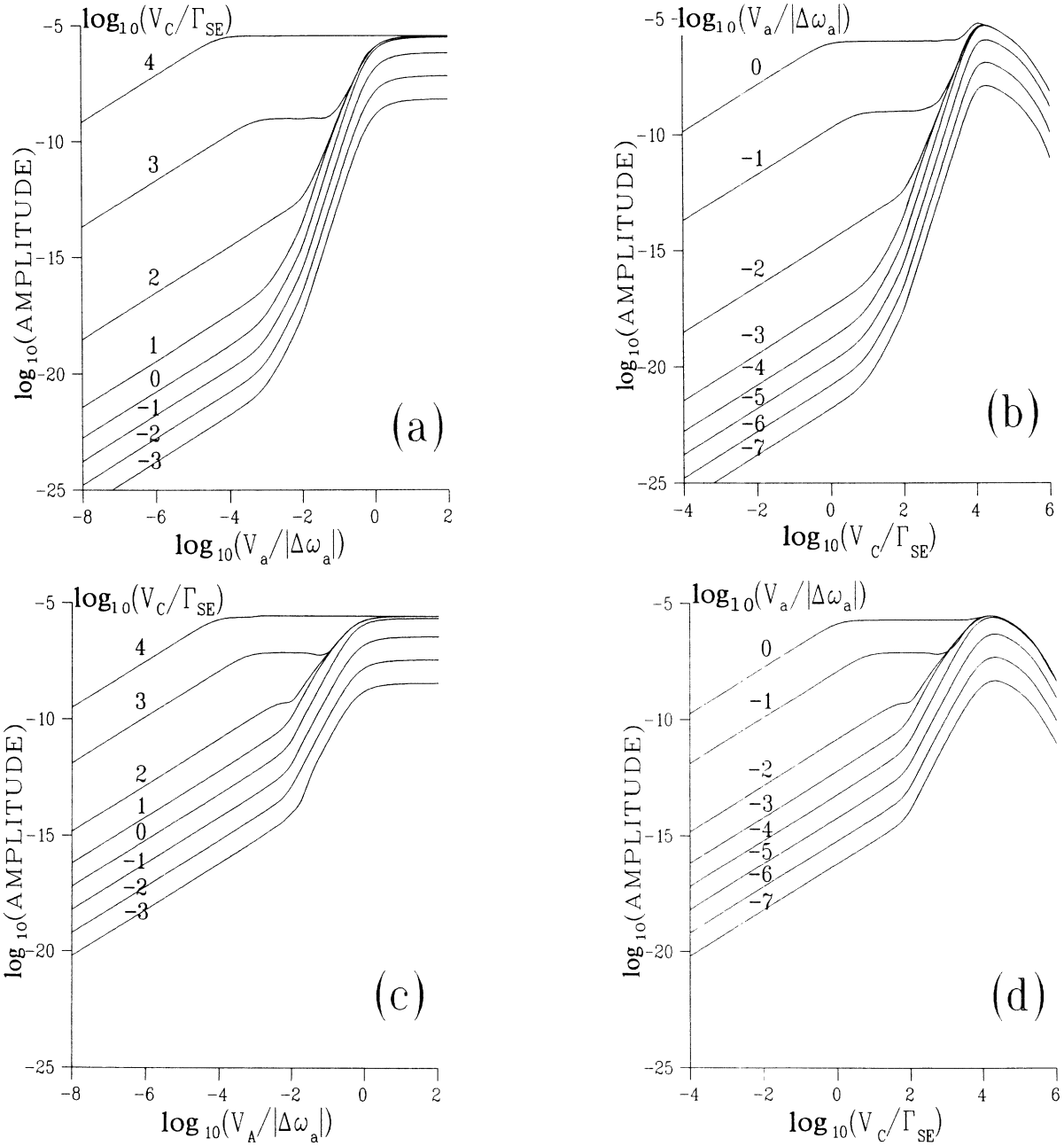

FIG. 7. The dependence of the amplitude on the strengths of the fields V_a and V_c for $\Delta\omega_a/\Gamma_{SE} = -10^4$. (a) Very low proper dephasing. The logarithm of the amplitude is shown as a function of the logarithm of $V_a/|\Delta\omega_a|$ for different values of V_c/Γ_{SE}. (b) Very low proper dephasing. The logarithm of the amplitude is shown as a function of the logarithm of V_c/Γ_{SE} for different values of $V_a/|\Delta\omega_a|$. (c) Same as (a) but for moderate proper dephasing ($\alpha P = \Gamma_{SE}/2$). (d) Same as (b) but for the same moderate proper dephasing.

and its detuning. The two new ground-state levels g_g and g_{ex} have a very different character for weak fields. One of them (g_g) is ground-state-like (i.e., populated) while the other one (g_{ex}) has the excited state character. As the field increases, mixing between the two is more pronounced, until at very strong fields (where most of the dressed states theories are analyzed) the two are completely equivalent. Here, since we are dealing with a FWM situation, one may consider the FWM process to start after the first photon dressed the levels. As shown in paper I, the extra resonance and the ordinary resonance both constitute the Rabi pair, starting off differently at low fields, to become equivalent at strong fields. Thus, the extra resonance is due to g_{ex}, the unpopulated split ground state. As the field increases, the population of this state increases, and the effective detunings of the ω_a and the ω_c fields are decreased, causing an increase in the strength of the FWM signal. The population in a dressed state is given by the standard Bloch equation result, which for the intermediate V_a field case behaves like V_a^2, while the level shifts depend on V_a. Since the level shift $\Delta\omega_a$ appears twice in the resonant denominator, the expected dependence on the V_a field is the fifth power, which is indeed observed in Fig. 7(a). Similar arguments will lead to the other observed power dependencies in Figs. 5–7.

The intermediate region can be addressed by looking at the relative value of V_c and V_a. The larger of the two determines which level shift is dominant, and the saturating intensity of the other field will change accordingly. Going back to Fig. 6(d), the first saturation plateau is described above, while the nonlinear region is reached for $V_a > V_c$. Here the role of the two fields is reversed, in analogy to the weak V_c case discussed above, leading to saturation at $V_a > \Delta\omega_a$. Thus, in these cases a double plateau behavior is observed, with the transition regions defined above.

VI. CONCLUSIONS

The calculation in this paper was performed, for convenience, for an OLS atom, but all the results are presented in normalized units. Thus, field strengths are presented in terms of either the detuning $\Delta\omega_a$ or the relevant linewidth (i.e., Γ_{jg}), and the comparison to real system (i.e., Na) should be possible.

For experiments done on the Na D lines, $\Gamma_{SE} \approx 10$ MHz, and the values of the parameters can be estimated. A pulsed laser experiment may achieve a Rabi frequency of order 1 cm^{-1}, which gives $V/\Gamma_{SE} \approx 10\,000$—the highest number used in our calculations. As detailed above, the perturbation limit applies for all fields being weak. For the c field, which is scanning through resonance, a weak field means $V_c/\Gamma_{SE} \ll 1$ (which for Na means intensities less than 1 mW/cm^2). Such intensities were not used in the original PIER 4 experiments,[18,26] and therefore the theory presented here is necessary for detailed pressure, power, and detuning dependence analysis, even though the perturbation approach is capable of predicting the existence and general features of the extra resonances.

The perturbation approach to extra resonances made the specific prediction that these are indeed extra resonances which disappear at zero pressure (or other proper dephasing mechanisms). A new prediction of the present theory is that even at zero pressure there exists a field-induced resonance. Moreover, at any field there is a pressure low enough so that the extra resonance is field induced rather than pressure induced. In the Na experiments where $\Gamma_{SE} \approx 10$ MHz for buffer-gas pressure above a few torr, $\alpha P/\Gamma_{SE} > 1$, the extra resonance is pressure broadened, its width is proportional to pressure, and its amplitude is constant, as observed in those experiments. When the PIER 4 integrated intensity was plotted against pressure, a nonzero intercept was observed, and in the linewidth versus pressure a residual width is also observed. Several factors may have contributed to these nonzero intercepts, including the fluctuation induced extra resonances due to the finite laser linewidth.[21] The observations are consistent with the predictions of the present paper, but additional experiments are needed to separate the various possible contributions to the signal at low pressures.

In paper I relaxations were not considered. As shown in this paper, that case is equivalent to the particular choice of proper dephasing being equal to the level lifetime ($T_2 = T_1$). This choice of dephasing rate does not affect the physical nature of the resonances, or the qualitative description of the process as given there. In particular, in that paper we identified the extra resonance as being a part of a Rabi pair with the ordinary resonance. We also predicted that when the strength of the third field is comparable to the Rabi splitting of the ordinary and extra resonances, stirring will occur, in analogy to other exchange narrowing phenomena. All these predictions are confirmed by the present calculation. The present, detailed calculation identifies the pressure and field strengths needed to see these (field-induced) effects. Experiments are under way in our laboratory to verify the predictions of the present paper.

ACKNOWLEDGMENTS

We wish to thank A. N. Weiszmann for help in formulating the original problem and many conversations about the present paper. Useful discussions with A. Wilson-Gordon, E. Ozizmir, K. Enad, G. Michalakis, L. Sartori, and P. Stern are gratefully acknowledged. We thank the Academic Computer Center of the College of Staten Island and the City University Computer center for their support. This work was supported in part by a grant from the Israel–U.S. Binational Science Foundation and by Grant No. 666470 from the C.U.N.Y.

APPENDIX A: APPLICATION OF THE FORMALISM TO A TWO-LEVEL SYSTEM

Consider a two-level system interacting with a monochromatic field of frequency ω. The excited state (2) decays spontaneously to the ground state (1) with the decay rate Γ_2. Thus the term feeding population into the

ground state is

$$\gamma_{21}=\Gamma_2 \tag{A1}$$

For this system, the rotating-wave approximation (RWA) Hamiltonian is

$$H=\hbar\begin{bmatrix}-\omega_0/2 & \bar{V}e^{i\omega t}\\ Ve^{-i\omega t} & \omega_0/2\end{bmatrix}, \tag{A2}$$

where ω_0 is the frequency separation between the levels. Referring to Eq. (2.7) and using the transformation

$$T(t)=\begin{bmatrix}e^{-i\omega t/2} & 0\\ 0 & e^{i\omega t/2}\end{bmatrix} \tag{A3}$$

one obtains

$$H'=\hbar\begin{bmatrix}\Delta\omega/2 & \bar{V}\\ \bar{V} & -\Delta\omega/2\end{bmatrix}. \tag{A4}$$

In Eq. (A4), $\Delta\omega$ is the detuning (i.e., $\Delta\omega=\omega-\omega_0$).

The steady-state matrix elements can be obtained by the method indicated in Eq. (2.17), where ρ' is defined in Eq. (2.5). Setting V real, one obtains

$$\rho_{11}^s=\tfrac{1}{2}+\Delta\rho\ , \tag{A5}$$

$$\rho_{22}^s=\tfrac{1}{2}-\Delta\rho\ , \tag{A6}$$

$$\Delta\rho=\frac{1}{2}\frac{[(\Delta\omega)^2+\Gamma_{12}^2]}{[(\Delta\omega)^2+4V^2\Gamma_{12}/\Gamma_2+\Gamma_{12}^2]}\ , \tag{A7}$$

$$\rho_{12}'^s=(\Delta\omega+i\Gamma_{12})\frac{V}{[(\Delta\omega)^2+4\Gamma_{12}/\Gamma_2V^2+\Gamma_{12}^2]}\ . \tag{A8}$$

The polarization at the frequency ω is

$$P_\omega=p_{12}\rho_{21}'^s\ , \tag{A9}$$

where $\rho_{21}'^s=\rho_{12}'^s$ is obtained from Eq. (A8).

A corresponding wave-function treatment, where at $t=0$ the system is assumed to be in its ground state, yields

$$P_{21}^s=\frac{2V^2}{[(\Delta\omega)^2+4V^2]}\ , \tag{A10}$$

$$P_{11}^s=1-P_{21}^s\ , \tag{A11}$$

where P_{11}^s and P_{21}^s are the steady-state populations in states 1 and 2, respectively. The expression obtained for the polarization at the frequency ω is

$$P_\omega=p_{12}\Delta\omega\frac{V}{[(\Delta\omega)^2+4V^2]}\ . \tag{A12}$$

The corresponding equations to be compared are Eq. (A10) with Eq. (A6), Eq. (A11) with Eq. (A5), and Eq. (A12) with the real part of Eq. (A8). The general features are similar. For instance, both sets of equations yield equal populations of $\frac{1}{2}$ for $V\to\infty$, the vanishing of the real part of P_ω exactly on resonance, and the vanishing of P_ω for $V\to\infty$. Certainly, however, the effects of the inclusion of decay manifest themselves even for large V/Γ. For instance, neglecting the Γ_{12}^2 in Eq. (A8), Eq. (A9) yields

$$\mathrm{Re}P_\omega=P_{12}\Delta\omega\frac{V}{[(\Delta\omega)^2+4\Gamma_{12}/\Gamma_2V^2]}\ . \tag{A13}$$

Comparison of Eqs. (A12) and (A13) shows that the expressions are equal for $\Gamma_{12}/\Gamma_2=1$. In the absence of proper dephasing, where the entire contribution to transverse relaxation comes from lifetimes, $\Gamma_{12}/\Gamma_2=\frac{1}{2}$. Thus the equivalence of the wave function and density-matrix formulations occur for a specific value of the proper dephasing.

APPENDIX B: THE SUPERMATRIX Z

The supermatrix Z is given by

$$\begin{bmatrix}
1 & 1 & 1 & 1 & 0 & 0 & 0 & 0 & 0 & 0 & 0 & 0 & 0 & 0 & 0 & 0\\
i\gamma_{12} & -i\Gamma_2 & i\gamma_{32} & i\gamma_{42} & 0 & 0 & 0 & -\bar{h}_{23} & -\bar{h}_{24} & 0 & 0 & 0 & 0 & h_{23} & h_{24} & 0\\
i\gamma_{13} & i\gamma_{23} & -i\Gamma_3 & i\gamma_{43} & 0 & \bar{h}_{13} & 0 & \bar{h}_{23} & 0 & 0 & 0 & -h_{13} & 0 & -h_{23} & 0 & 0\\
i\gamma_{14} & i\gamma_{24} & i\gamma_{34} & -i\Gamma_4 & 0 & 0 & \bar{h}_{14} & 0 & \bar{h}_{24} & 0 & 0 & 0 & -h_{14} & 0 & -h_{24} & 0\\
0 & 0 & 0 & 0 & G_{12} & -\bar{h}_{23} & -\bar{h}_{24} & 0 & 0 & 0 & 0 & 0 & 0 & h_{13} & h_{14} & 0\\
-h_{13} & 0 & h_{13} & 0 & -h_{23} & G_{13} & 0 & 0 & 0 & 0 & 0 & 0 & 0 & 0 & 0 & h_{14}\\
-h_{14} & 0 & 0 & h_{14} & -h_{24} & 0 & G_{14} & 0 & 0 & h_{13} & 0 & 0 & 0 & 0 & 0 & 0\\
0 & -h_{23} & h_{23} & 0 & 0 & 0 & 0 & G_{23} & 0 & 0 & h_{13} & 0 & 0 & 0 & 0 & h_{24}\\
0 & -h_{24} & 0 & h_{24} & 0 & 0 & 0 & 0 & G_{24} & h_{23} & -h_{14} & 0 & 0 & 0 & 0 & 0\\
0 & 0 & 0 & 0 & 0 & 0 & \bar{h}_{13} & 0 & \bar{h}_{23} & G_{34} & 0 & -h_{14} & 0 & -h_{24} & 0 & 0\\
0 & 0 & 0 & 0 & 0 & 0 & 0 & -\bar{h}_{13} & -\bar{h}_{14} & 0 & G_{21} & h_{23} & h_{24} & 0 & 0 & 0\\
\bar{h}_{13} & 0 & -\bar{h}_{13} & 0 & 0 & 0 & 0 & 0 & 0 & -\bar{h}_{14} & h_{23} & G_{31} & 0 & 0 & 0 & 0\\
\bar{h}_{14} & 0 & 0 & -\bar{h}_{14} & 0 & 0 & 0 & 0 & 0 & 0 & \bar{h}_{24} & 0 & G_{41} & 0 & 0 & -h_{13}\\
0 & \bar{h}_{23} & -\bar{h}_{23} & 0 & \bar{h}_{13} & 0 & 0 & 0 & 0 & -\bar{h}_{24} & 0 & 0 & 0 & G_{32} & 0 & 0\\
0 & \bar{h}_{24} & 0 & -\bar{h}_{24} & \bar{h}_{14} & 0 & 0 & 0 & 0 & 0 & 0 & 0 & 0 & 0 & G_{42} & -\bar{h}_{23}\\
0 & 0 & 0 & 0 & 0 & \bar{h}_{14} & 0 & \bar{h}_{24} & 0 & 0 & 0 & 0 & -h_{13} & 0 & -h_{23} & G_{43}
\end{bmatrix}$$

where $G_{lm}=h_{ll}-h_{mm}-i\Gamma_{lm}$.

[1]N. Bloembergen, *Nonlinear Optics* (Benjamin, New York, 1965).

[2]Y. R. Shen, *Principles of Nonlinear Optics* (Wiley, New York, 1984).

[3]N. Bloembergen and Y. R. Shen, Phys. Rev. **133**, 210 (1964).

[4]D. J. Harter, and R. W. Boyd, IEEE J. Quantum Electron. **QE-16**, 1126 (1980); R. W. Boyd, M. G. Raymer, P. Narum, and D. J. Harter, Phys. Rev. A **24**, 411 (1981); D. J. Harter, P. Narum, M. G. Raymer, and R. W. Boyd, Phys. Rev. Lett. **46**, 1192 (1981) D. J. Harter and R. W. Boyd, Phys. Rev. A **29**, 739 (1984).

[5]F. A. M. de Oliveria, Cid B. de Araujo, and J. R. Rios Leite, Phys. Rev. A **25**, 2430 (1982).

[6]G. S. Agarwal and N. Nayak, J. Opt. Soc. Am. B **1**, 164 (1984); G. P. Agarwal, Phys. Rev. A **28**, 2286 (1983).

[7]K. F. Freed, J. Chem. Phys. **43**, 1113 (1965).

[8]L. R. Wilcox and W. E. Lamb, Jr., Phys. Rev. **119**, 1915 (1960).

[9]B. Dick and R. M. Hochstrasser, Chem. Phys. **75**, 133 (1983).

[10]A. M. Levine, W. M. Schreiber, and A. N. Weiszmann, Phys. Rev. A **25**, 625 (1982).

[11]A. D. Wilson-Gordon, R. Klimovsky-Barid, and H. Friedmann, Phys. Rev. A **25**, 1580 (1982); A. D. Wilson-Gordon and H. Friedmann, *ibid.* **30**, 1377 (1984); H. Friedmann, A. D. Wilson-Gordon, and M. Rosenbluh, *ibid.* **33**, 1783 (1986).

[12]H. Friedmann and A. D. Wilson-Gordon, Phys. Rev. A **26**, 2768 (1982); **28**, 302 (1983).

[13]P. R. Berman and R. Salomaa, Phys. Rev. A **25**, 2667 (1982).

[14]T. A. DeTemple, M. K. Gurnick, and F. H. Julien, Phys. Rev. A **37**, 3358 (1988).

[15]A. M. Fernando de Oliveira, Cid. B. de Araujo, and Jose R. Rios Leite, Phys. Rev. A **38**, 5688 (1988).

[16]A. M. Levine, N. Chencinski, W. M. Schreiber, A. N. Weiszmann, and Yehiam Prior, Phys. Rev. A **35**, 2550 (1987).

[17]L. Allen and J. H. Eberly, *Optical Resonance and Two Level Atoms* (Wiley, New York, 1975); A. Abragam, *Principles of Nuclear Magnetism* (Oxford University Press, London, 1961).

[18]Yehiam Prior, A. Bogdan, M. Dagenais, and N. Bloembergen, Phys. Rev. Lett. **46**, 111 (1981).

[19]J. R. Andrews and R. M. Hochstrasser, Chem. Phys. Lett. **83**, 427 (1981); J. R. Andrews, R. M. Hochstrasser, and H. P. Trommsdorf, Chem. Phys. **62**, 87 (1981).

[20]G. Grynberg, M. Pinard, and P. Verkerk, Opt. Commun. **50**, 261 (1984).

[21]Yehiam Prior, I. Schek, and J. Jortner, Phys. Rev. A **31**, 3775 (1985); A. G. Kofman, A. M. Levine, and Yehiam Prior, Phys. Rev. A **37**, 1248 (1988).

[22]L. Rothberg, *Progress in Optics XXIV*, edited by E. Wolf (North-Holland, Amsterdam, 1987), p. 41.

[23]Y. Prior, IEEE J. Quantum Electron. **QE-20**, 37 (1984).

[24]S. Stenholm, *Foundation of Laser Spectroscopy* (Wiley, New York, 1984).

[25]C. Cohen-Tannoudji and S. Reynaud, J. Phys. B **10**, 345 (1977); **10**, 365 (1977).

[26]A. Bogdan, Ph.D. thesis, Harvard University, 1981.